The *Swift* Discovery of X-ray Afterglows Accompanying Short Bursts from SGR 1900+14

Y. E. Nakagawa,[1,2] T. Sakamoto,[3,4] G. Sato,[3] N. Gehrels,[3] K. Hurley,[5] AND D. M. Palmer,[6]

ABSTRACT

The discovery of X-ray afterglows accompanying two short bursts from SGR 1900+14 is presented. The afterglow luminosities at the end of each observation are lower by 30-50% than their initial luminosities, and decay with power law indices $p \sim$ 0.2-0.4. Their initial bolometric luminosities are $L \sim 10^{34}$-$10^{35}\,\mathrm{erg\,s^{-1}}$. We discuss analogies and differences between the X-ray afterglows of SGR short bursts and short gamma-ray bursts.

Subject headings: stars: neutron – stars: pulsars: individual(SGR 1900+14)

1. Introduction

Soft gamma repeaters (SGRs) are intriguing sources of very energetic (super-Eddington luminosity) high energy bursts. They exhibit repetitive, sporadic bursting activity with typical burst durations of $\sim 100\,\mathrm{ms}$ (e.g., Woods & Thompson 2006). Four have been identified as definite SGRs, three are candidate SGRs, and the X-ray source AX J1818.8$-$1559 is either a candidate SGR or an anomalous X-ray pulsar (AXP) (Mereghetti et al. 2007; Nakagawa et al. 2007b). Quiescent X-ray emission has been observed from SGRs with a flux which exceeds the Eddington luminosity (Nakagawa et al. 2007b). The energy reservoir for the

[1]Graduate School of Science and Engineering, Aoyama Gakuin University, Sagamihara, Kanagawa 229-8558, Japan

[2]Institute of Physical and Chemical Research (RIKEN), 2-1 Hirosawa, Wako, Saitama 351-0198, Japan

[3]NASA Goddard Space Flight Center, Greenbelt, MD 20771

[4]University of Maryland, Baltimore County, 1000 Hilltop Circle, Baltimore, MD 21250

[5]Space Sciences Laboratory, 7 Gauss Way, University of California, Berkeley, CA 94720-7450

[6]Los Alamos National Laboratory, P.O.Box 1663, Los Alamos, NM 87545

bursts and the steady emission is generally believed to be magnetic energy dissipation in the framework of the magnetar model (Duncan & Thompson 1992; Paczyński 1992; Thompson & Duncan 1995, 1996).

Among the SGR bursts, there is a minority population with a few seconds duration known as intermediate bursts (e.g., Olive et al. 2004). Some of the intermediate duration bursts from SGR 1900+14 have an X-ray tail with a duration of a few thousand seconds that is interpreted as a part of the burst itself (Lenters et al. 2003). More rarely, giant flares occur with an initial short, intense spike, several hundred milliseconds long, followed by a long pulsating tail lasting a few hundred seconds; these are the most exotic magnetar phenomena. A large flare from SGR 1900+14 on 2001 April 18 displayed an X-ray afterglow lasting about 11 days (Feroci et al. 2003). Radio afterglows were observed after the giant flares from SGR 1900+14 on 1998 August 27 and from SGR 1806−20 on 2004 December 27 (Frail et al. 1999; Cameron et al. 2005). Indeed it is possible that some short-duration cosmic gamma-ray bursts (GRBs) could actually be extragalactic giant magnetar flares (Hurley et al. 2005). Radio, optical, and/or X-ray afterglows are a common phenomenon for the long-duration GRBs (typical durations of 2 seconds or more), but they have only been observed for 13 of 20 GRBs of duration less than 2 seconds (hereafter short GRBs). In addition, a flux increase and a slow decay of the quiescent emission ($F \propto t^{-0.3}$ over 110 days, where F is the flux and t is the time since the burst) has been observed after a short burst from the AXP CXOU J164710.2-455216 (Campana & Israel 2006; Israel et al. 2007; Nakagawa et al. 2007b). A flux increase and a decay having two different components ($F \propto t^{-4.8\pm0.5}$ for $t < 0.5\,\mathrm{day}$ and $F \propto t^{-0.22\pm0.01}$ for $t \gtrsim 0.5\,\mathrm{day}$) has been observed in the quiescent emission after an outburst from AXP 1E 2259+586 in 2002 (Woods et al. 2004).

Many bursts from the known SGRs have been detected by *Swift* (Gehrels et al. 2004) because of the very wide field-of-view and excellent sensitivity of the Burst Alert Telescope (BAT; Barthelmy et al. 2005). Thanks to the prompt, precise localization by the BAT, and the fast slew capability of *Swift*, X-ray follow-up observations by the X-ray Telescope (XRT; Burrows et al. 2005) have taken place soon after short bursts from SGR 1900+14. In this paper, we report the *Swift* discovery of X-ray afterglows from three of these short bursts. We present spectral analyses of the bursts and the X-ray afterglow using BAT and XRT data. We discuss analogies and differences between the short bursts from the SGRs and the short cosmic GRBs. Despite many satellite and ground-based telescope observations, the distance to SGR 1900+14 still remains very uncertain. In this paper, the distance is assumed to be 10 kpc (Hurley et al. 1999; Vrba et al. 2000).

2. Data Analysis

2.1. Observations

Prompt follow-up observations by the *Swift* XRT were performed for three short bursts from SGR 1900+14 detected by the *Swift* BAT. They were detected on 2006 April 14 (trigger number 205164), 2006 June 10 (trigger number 214277) and 2006 November 26 (trigger number 240801). Figure 1 shows their BAT light curves. In this paper, we will call these bursts A, B and C, respectively. Their main properties are summarized in table 1. The T_{90} durations of these bursts are all ~ 40 ms. Note that the BAT and XRT observations were not simultaneous.

2.2. Data Reduction

We used the standard BAT software (HEASoft 6.3.2) and the latest calibration database (CALDB: 20070924) to process the BAT event data. The burst pipeline script, `batgrbproduct` (v2.39), was used for the processing. Because the bursts were short and weak, `batgrbproduct` failed to find the burst intervals, and we used the time interval determined by the flight software for creating the spectra. `XSPEC 12.3.1` was used to fit the spectrum (Arnaud 1996). The BAT spectral analyses were performed in the 15-100 keV band.

The XRT data were systematically analyzed using the pipeline script. The cleaned event data from the Window Timing (WT) and Photon Counting (PC) modes from the *Swift* Science Data Center (SDC) were used. Although both WT and PC mode data were processed in the pipeline, hereafter we focus only on the PC mode data. The search for the X-ray counterpart, construction of the X-ray light curve, and fitting the X-ray light curve and spectra were performed automatically using the standard XRT softwares and calibration database (HEAsoft 6.3.2 and CALDB: 20070730). The source region was selected to be a circle of $47''$ radius. The background region was an annulus of outer radius $150''$ and inner radius $70''$ excluding the background X-ray sources detected by `ximage`. Since the count rate in the PC mode was less than $0.1\,\mathrm{counts\,s^{-1}}$, no pile-up correction was applied in the processing. The light curve was binned based on the number of photons required to meet at least a 10σ criterion in each bin. The ancillary response function (ARF) files were created by `xrtmkarf` (v0.5.5). The spectra were binned to at least 20 counts in each spectral bin by `grppha`. The XRT spectral analyses were performed in the 0.3-10 keV band.

2.3.   Spectral Analysis

Since a two blackbody function (2BB) has been suggested as the most acceptable model for the two SGRs 1806−20 and 1900+14 using HETE-2 data (Nakagawa et al. 2007a), 2BB was used for the spectral analysis of the short bursts from SGR 1900+14 detected by the BAT. If reliable spectral parameters were not obtained, a single blackbody model (BB) was used instead. Because we performed the spectral fits using the energy range above 15 keV, an absorption model was not applied.

The spectral parameters for the SGR short bursts are summarized in table 2. The spectra of bursts A and C are well reproduced by the 2BB model, and their spectral parameters are consistent with typical values found previously (Nakagawa et al. 2007a). For burst B, BB gives an acceptable result. The unabsorbed bolometric luminosities using the spectral parameters for 2BB and BB are also summarized in table 2.

For spectral analysis of the XRT data, 2BB and a blackbody plus a power law model (BB+PL) were used. If reliable spectral parameters were not obtained, BB and a power law model (PL) were also used. Since a reliable value of the absorption model was not determined for some observations, the value was fixed to $1.91 \times 10^{22} \, \mathrm{cm}^{-2}$, derived from XMM-Newton observations (Mereghetti et al. 2006).

The results of the XRT spectral analysis are summarized in table 3. The decreasing trend of burst A is well reproduced by the 2BB and BB+PL models. For bursts B and C, BB and PL give acceptable results.

2.4.   Light Curves

To derive light curves of the unabsorbed bolometric luminosity, a conversion factor from count rate to luminosity was calculated using the 2BB or BB time-averaged luminosity, and a time averaged XRT count rate. In figure 2, the X-ray light curves are shown with the luminosities of their preceding short bursts. Since there are not enough statistics to produce a light curve for burst B, this event is not considered further.

As seen in figure 2, there is a clear decay in the X-ray emission. The luminosities at the end of each observation are 30-50% lower than the initial X-ray luminosities. Fitting the light curve with a power law model ($L \propto t^{-p}$, where L is the luminosity, t is the time since the burst, and p is the decay index), the best fit decay index is 0.2±0.1 for burst A. Since there are only two data points for burst C, we calculate the decay index which passes through the two data points and find 0.4. The slopes are plotted as dashed lines in figure 2.

These decreasing trends can be interpreted as the X-ray afterglows following the short SGR bursts.

The upper panel in figure 3 shows the quiescent X-ray light curve during periods when SGR 1900+14 was emitting short bursts, while the lower panel presents the burst rates [1]. Note the activity at MJD = 53823 days (2006 March 29); 40 bursts were detected in that one day. Bursts A, B and C were detected after that active day. Therefore, we believe that the X-ray emission which we discovered is not related to the enhanced activity of the SGR.

3.   Discussion and Conclusions

As shown in figure 2, the luminosities of the SGR short bursts are two or three orders of magnitude larger than the backwards-extrapolated values from the SGR X-ray afterglows. This implies that the decreasing SGR X-ray afterglow is not the tail of the short bursts. Therefore this result is different from the X-ray emission accompanying intermediate bursts from SGR 1900+14, which is interpreted as the tail of the burst itself (Lenters et al. 2003). Also, compared with the afterglow of the large flare from SGR 1900+14 (Feroci et al. 2003), or with the moderate flux decay of AXP CXOU J164710.2−455216 (Campana & Israel 2006; Nakagawa et al. 2007b), the decay time scale of the afterglow accompanying the SGR short bursts (that is, the time to decrease by a factor of ~ 2) is shorter by a factor of ~ 3. Since the observing period of the SGR X-ray afterglow ($t < 0.5$ day) is different from that of the moderate flux decay of AXP CXOU J164710.2−455216 ($t \gtrsim 0.5$ day), the decay indices and time scales are not exactly comparable. The initial ($t < 0.5$ day) decay index $p = 4.8 \pm 0.5$ of AXP 1E 2259+586 is much steeper than that of the SGR X-ray afterglow, despite the fact that the time scale of the flux decay of AXP 1E 2259+586 (Woods et al. 2004) is consistent with the decay time scale of the SGR X-ray afterglow (same definition as above). This suggests that the X-ray afterglows of the short bursts might be a different phenomenon. Note that the decay indeces at 0.5 day after the bursts for the two AXPs CXOU J164710.2−455216 ($p = -0.3$) and 1E 2259+586 ($p = -0.22$) are both consistent with the decay index of the SGR X-ray afterglow.

Here, we discuss the analogies and differences between the X-ray afterglows of short bursts from SGR 1900+14 and the X-ray afterglows of short GRBs. The decay indices of the SGR X-ray afterglows, p =0.2-0.4 (see § 2.4 and table 1), are similar to those of the two short GRBs 050724 ($p = 0.6 \pm 0.2$; Campana et al. 2006) and 051221A ($p = 0.04^{+0.27}_{-0.21}$; Burrows et al. 2006). On the other hand, the five short GRBs 050509B ($p = 1.10^{+1.26}_{-0.53}$; Gehrels et

---

[1]The burst rate is derived from http://www.ssl.berkeley.edu/ipn3/sgrlist.txt.

2005), 050709 ($p \gtrsim 1$; Fox et al. 2005), 051210 ($p = 2.58 \pm 0.11$; Parola et al. 2007), 060313 ($p = 1.46 \pm 0.08$; Roming et al. 2006) and 061201 ($p = 1.90 \pm 0.15$; Stratta et al. 2007) have much steeper temporal indices than those of the SGR X-ray afterglows. The X-ray afterglow luminosities of the SGR short bursts are $L \sim 10^{34}$-$10^{35}\,\mathrm{erg\,s^{-1}}$. Considering the cosmological distances to the short GRBs, the SGR X-ray afterglow luminosity is lower by a factor of 10^{6}-10^{12} than the luminosities of the four short GRBs 050509B, 050709, 050724 and 051221A (see the following literature for their redshifts; Berger & Soderberg 2005; Prochaska et al. 2005; Bloom et al. 2006; Covino et al. 2006). For the other three GRBs, secure redshift measurements have not been reported yet. Thus the indices of the X-ray afterglows of GRBs 050724 and 051221A are similar to those of the SGR X-ray afterglows, while the luminosities are different.

Considering the super-Eddington luminosities of the short bursts ($L \gtrsim 10L_{\mathrm{Edd}}$ where $L_{\mathrm{Edd}} = 1.8 \times 10^{38}\,\mathrm{erg\,s^{-1}}$ is the Eddington luminosity with $M = 1.4M_{\odot}$ and $R = 10\,\mathrm{km}$), one possible explanation for the SGR X-ray afterglows might be a mechanism similar to an external shock in a GRB. That is, the short burst might be generated by a relativistic jet from a neutron star, and an interaction between the jet and an interstellar medium would generate the afterglow. The lower limit to the number density around SGR 1900+14 $n \gtrsim 0.6(N_{\mathrm{H}}/1.91 \times 10^{22}\,\mathrm{cm^{-2}})(d/3 \times 10^{22}\,\mathrm{cm})^{-1}\,\mathrm{cm^{-3}}$ (where d is the distance to SGR 1900+14) is reasonable to produce the SGR X-ray afterglow considering the number density for GRBs (Sari, Piran & Narayan 1998). We can estimate a bulk Lorentz factor assuming a total released energy $E \sim T_{90}L \sim 7.6 \times 10^{38}\,\mathrm{erg}$ for Burst C and $n \sim 1\,\mathrm{cm^{-3}}$ (Fenimore et al. 1996). The velocity of the material which is responsible for the external shock emission might be a weakly relativistic jet with $\gamma \sim 2$ at 1000 s after the short burst. Another possibility might be emission from the plasma remaining after the short burst, or an intrinsic quiescent X-ray flux increase. An alternative simple possibility might be the cooling of the surface heated by the plasma of the short burst (Thompson et al. 2002). Although some models have been proposed to explain the afterglows accompanying giant flares (Yamazaki et al. 2005; Lyutikov 2006; Cea 2006), it is not clear that these models can produce the afterglow emission from short SGR bursts. The presence of these afterglows may imply that short burst activity is in fact much longer than it appears to be. Indeed, X-ray afterglow emission accompanying short SGR bursts could be a key to understanding the origin and emission mechanism of these bursts. Further prompt multi-wavelength observations of these afterglows are needed to understand the radiation process.

Facilities: Swift (BAT), Swift (XRT).

REFERENCES

Arnaud, K. A. 1996, in Astronomical Data Analysis Software and Systems V, eds. G. Jacoby and J. Barnes, ASP Conference Series, 101, 17

Barthelmy, S. D. et al., 2005, Space Sci. Rev., 120, 143

Berger, E., & Soderberg, A. M. et al., 2005, GRB Coord. Netw. Circ., 4384

Bloom, J. S. et al., 2006, ApJ, 638, 354

Burrows, D. N. et al., 2005, Space Sci. Rev., 120, 165

Burrows, D. N. et al., 2006, arXiv: astro-ph/0604320

Cameron, P. B. et al., 2005, Nature, 434, 1112

Campana, S., & Israel G. L. 2006, The Astronomer's Telegram, 893

Campana, S. et al. 2006, A&A, 454, 113

Cea, P. 2006, A&A, 450, 199

Covino, S. et al. 2006, A&A, 447, L5

Duncan, R., & Thompson, C. 1992, ApJ, 392, L9

Fenimore, E. E., Madras, C. D., & Nayakshin, S. 1996, ApJ, 473, 998

Feroci, M. et al., 2003, ApJ, 596, 470

Fox, D. B. et al., 2005, Nature, 437, 845

Frail, D. A., Kulkarni, S. R., & Bloom, J. S. 1999, Nature, 398, 127

Gehrels, N. et al., 2004, ApJ, 611, 1005

Gehrels, N. et al., 2005, Nature, 437, 1038

Hurley, K. et al., 1999, ApJ, 510, L111

Hurley, K. et al., 2005, Nature, 434, 1098

Israel, G. L. et al., 2007, ApJ, 664, 448

Lenters, G. T. et al., 2003, ApJ, 587, 761

Lyutkov, M. 2006, MNRAS, 367, 1594

Mereghetti, S. et al., 2006, ApJ, 653, 1423

Mereghetti, S., Paizis, A., Gotz, D., Petry, D., Shaw, S., Beck, M., & Borkowski J. 2007, GRB Coord. Netw. Circ., 6927

Nakagawa, Y. E. et al., 2007a, PASJ, 59, 653

Nakagawa, Y. E., Yoshida, A., Yamaoka, K., & Shibazaki, N. 2007b, arXiv: astro-ph/0710.3816

Nousek, J. A. et al., 2006, ApJ, 642, 389

Olive, J.-F. et al., 2004, ApJ, 616, 1148

Paczyński, B. 1992, Acta Astron., 42, 145

La Parola, V. et al. 2007, arXiv: astro-ph/0701818

Prochaska, J. X. et al., 2005, GRB Coord. Netw. Circ., 3700

Roming, P. W. A. et al., 2006, arXiv: astro-ph/0605005

Sari, R., Piran, T., & Narayan, R. 1998, ApJ, 497, L17

Stratta, G. et al., 2007, A&A, 474, 827

Thompson, C., & Duncan, R. 1995, MNRAS, 275, 255

Thompson, C., & Duncan, R. 1996, ApJ, 473, 322

Thompson, C., Lyutikov, M., & Kulkarni, S. R. 2002, ApJ, 574, 332

Vrba, F. J., Henden, A. A., Luginbuhl, C. B., Guetter, H. H., Hartmann, D. H., & Klose, S. 2000, ApJ, 533, L17

Woods, P. M., et al., 2004, ApJ, 605, 378

Woods, P. M., & Thompson, C. 2006, in Compact Stellar X-ray Sources, ed. W. Lewin & M. van der Klis (Cambridge: Cambridge Univ. Press), 547

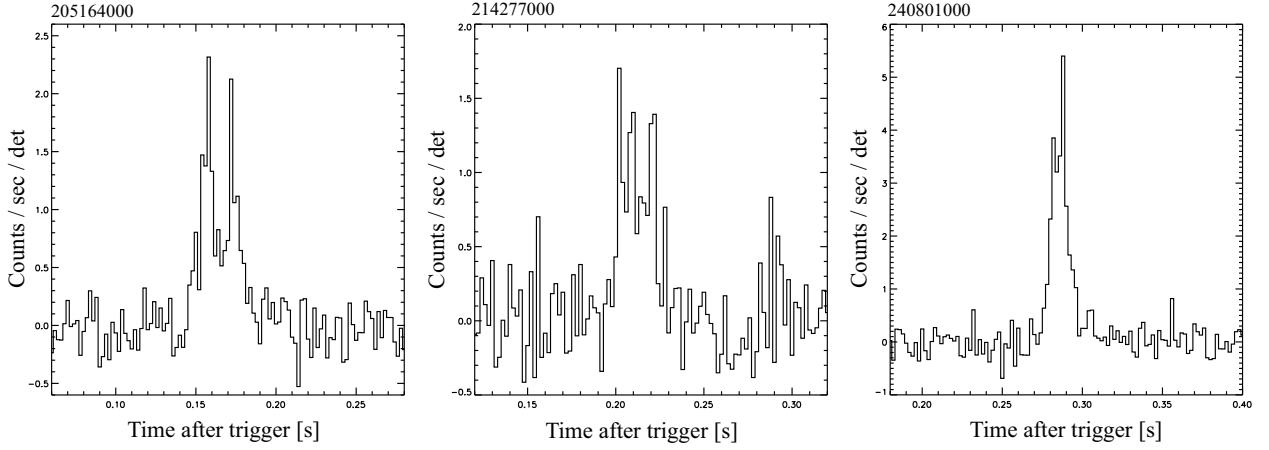Yamazaki, R., Ioka, K., Takahara, F., & Shibazaki, N., PASJ, 57, L11

Fig. 1.— 15-100 keV light curves for the short bursts from SGR 1900+14 detected by the *Swift* BAT.
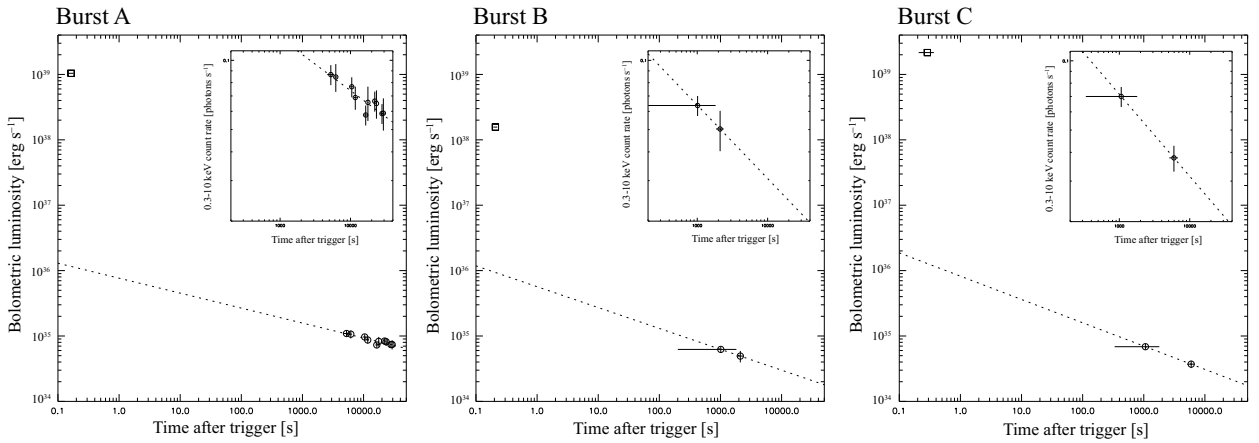

Fig. 2.— Afterglow light curve luminosity for burst A (*left*), B (*middle*) and C (*right*). The burst luminosities are indicated by the squares. The dashed lines indicate the extrapolation to the time of the burst. Inset: light curve in photons, with no spectral correction.
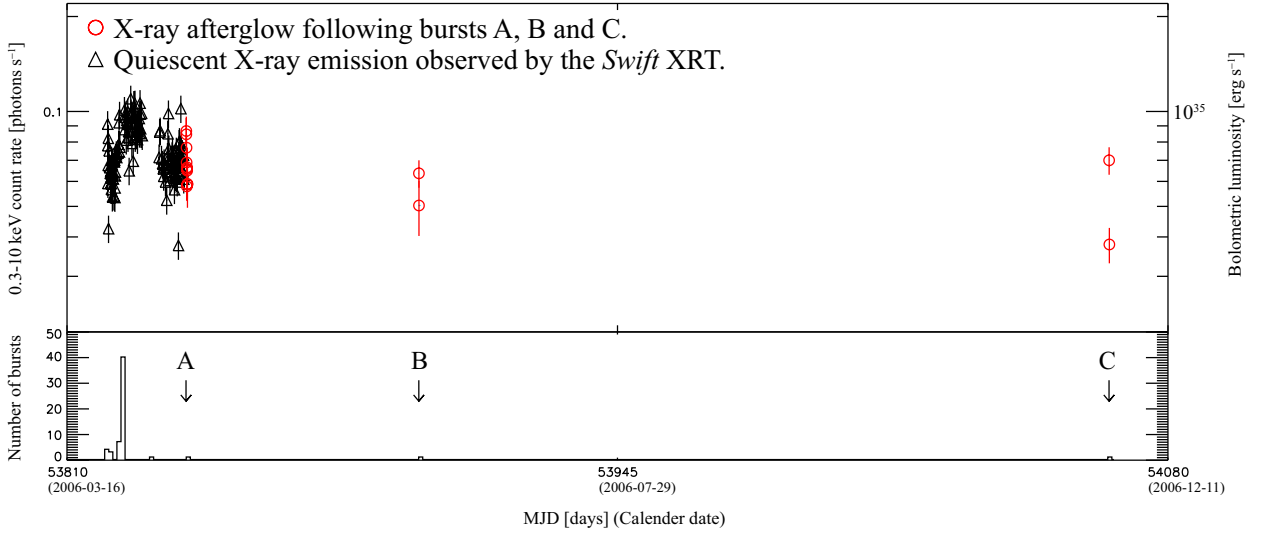
Fig. 3.— Upper panel: Quiescent X-ray emission from SGR 1900+14 observed during *Swift* XRT pointed observations (black triangles) and X-ray afterglow emission (red circles). Lower panel: Bursting history of SGR 1900+14 in bursts per day. The three events studied here are indicated by A, B and C.

Table 1: Main properties of three short bursts from SGR 1900+14 observed by *Swift*.

Burst	TrigNum[a]	Trigger time (UT)	T_{90} duration[b]	XRT Exposure Time (PC)	p[c]
			(ms)	(ks)	
A	205164	2006:04:14.04:35:29	34 ± 9	11.6	0.2 ± 0.1
B	214277	2006:06:10.06:53:01	38 ± 18	1.9	$\cdots$
C	240801	2006:11:26.13:16:08	40 ± 14	1.6	0.4

[a]*Swift* trigger number.

[b]T_{90} is the time to accumulate between 5% and 95% of the observed photons.

[c]p is the X-ray afterglow decay power law index with 90% confidence level uncertainties.

Table 2.　Spectral parameters of three short bursts from SGR 1900+14 observed by the *Swift* BAT.

Burst	Model	kT_{LT}[a] or kT_{BB}[b] (keV)	R_{LT}[c] or R_{BB}[b] (km)	kT_{HT}[a] (keV)	R_{HT}[c] (km)	L[d]	χ^2 (d.o.f.)
A	2BB	$3.6^{+2.2}_{-1.6}$	13^{+69}_{-9}	15^{+6}_{-3}	$0.8^{+0.6}_{-0.4}$	$7.4^{+10.5}_{-2.1}$	39 (34)
B	BB	$9.2^{+2.7}_{-2.2}$	$2.2^{+1.6}_{-0.9}$	$\cdots$	$\cdots$	$4.4^{+1.0}_{-1.1}$	18 (16)
C	2BB	$4.9^{+1.3}_{-1.2}$	13^{+11}_{-5}	13^{+10}_{-4}	1.3 ± 1.0	$19.0^{+4.9}_{-5.5}$	24 (34)

[a]kT_{LT} and kT_{HT} denote blackbody temperatures for the 2BB fit with 90% confidence level uncertainties.

[b]kT_{BB} and R_{BB} denote blackbody temperature and radius for the BB fit with 90% confidence level uncertainties.

[c]R_{LT} and R_{HT} denote blackbody radii of the 2BB fit with 90% confidence level uncertainties.

[d]L denotes the bolometric luminosity in units of $10^{39}\,\mathrm{erg\,s^{-1}}$ with 90% confidence level uncertainties.

Table 3.　Spectral parameters of observations after short bursts from SGR 1900+14 by the *Swift* XRT.

Burst	Model	N_H[a]	kT_{LT}[b] or kT_{BB}[c] (keV)	R_{LT}[d] or R_{BB}[c] (km)	kT_{HT}[b] (keV)	R_{HT}[d] (km)	Γ[e]	L[f]	χ^2 (d.o.f.)
A	2BB	1.91	0.5 ± 0.1	3 ± 1	$1.3^{+0.6}_{-0.3}$	0.3 ± 0.2	$\cdots$	1.0 ± 0.2	28 (34)
	BB+PL	1.91	$0.55^{+0.05}_{-0.06}$	$2.1^{+0.6}_{-0.8}$	$\cdots$	$\cdots$	$1.8^{+0.5}_{-1.1}$	$5.6^{+6.2}_{-4.2}$	31 (35)
B	BB	1.91	0.7 ± 0.1	$1.4^{+0.5}_{-0.4}$	$\cdots$	$\cdots$	$\cdots$	0.8 ± 0.1	5 (4)
	PL	1.91	$\cdots$	$\cdots$	$\cdots$	$\cdots$	2.2 ± 0.3	$2.4^{+1.0}_{-0.8}$	3 (4)
C	BB	1.91	0.7 ± 0.1	$1.5^{+0.6}_{-0.5}$	$\cdots$	$\cdots$	$\cdots$	0.6 ± 0.1	2 (5)
	PL	1.91	$\cdots$	$\cdots$	$\cdots$	$\cdots$	$2.5^{+0.6}_{-0.5}$	$1.2^{+0.9}_{-0.6}$	5 (5)

[a]N_H denotes the absorption. The value of N_H is fixed to $1.91 \times 10^{22}\,\mathrm{cm^{-2}}$ which is derived from XMM-Newton observations (Mereghetti et al. 2006).

[b]kT_{LT} and kT_{HT} denote blackbody temperatures of the 2BB fit with 90% confidence level uncertainties.

[c]kT_{BB} and R_{BB} denote blackbody temperature and radius for the BB+PL or BB fits with 90% confidence level uncertainties.

[d]R_{HT} and R_{HT} denote blackbody radii of the 2BB fit with 90% confidence level uncertainties.

[e]Γ denotes the power law index of the BB+PL or PL fits with 90% confidence level uncertainties.

[f]L denotes the bolometric luminosity in units of $10^{35}\,\mathrm{erg\,s^{-1}}$ with 90% confidence level uncertainties.